

---

# Spiking Deep Residual Network

---

**Yangfan Hu**  
Zhejiang University  
huyangfan@zju.edu.cn

**Huajin Tang**  
Sichuan University  
htang@scu.edu.cn

**Yueming Wang**  
Zhejiang University  
ymingwang@zju.edu.cn

**Gang Pan**  
Zhejiang University  
gpan@zju.edu.cn

## Abstract

Recently, spiking neural network (SNN) has received significant attentions for its biological plausibility. SNN theoretically has at least the same computational power as traditional artificial neural networks (ANNs), and it has the potential to achieve revolutionary energy-efficiency. However, at current stage, it is still a big challenge to train a very deep SNN. In this paper, we propose an efficient approach to build a spiking version of deep residual network (ResNet), which represents the state-of-the-art convolutional neural networks (CNNs). We employ the idea of converting a trained ResNet to a network of spiking neurons named Spiking ResNet. To address the conversion problem, we propose a shortcut normalisation mechanism to appropriately scale continuous-valued activations to match firing rates in SNN, and a layer-wise error compensation approach to reduce the error caused by discretisation. Experimental results on MNIST, CIFAR-10, and CIFAR-100 demonstrate that the proposed Spiking ResNet yields the state-of-the-art performance of SNNs.

## 1 Introduction

It has been shown that spiking neural network (SNN) [21] is the solution to bridge the gap between performance and computational costs and theoretically, SNN can approximate any function as ANNs. Unlike conventional ANN, neurons in SNN communicate with each other via discrete events (spikes) instead of continuous-valued activations. Such system is updated asynchronously as event arrives, thus reducing number of operations required at each time step. Recent developments show that SNN can be emulated by neuromorphic hardware such as TrueNorth [24], SpiNNaker [9] and Rolls [26] with several orders of magnitude less energy consumption than by contemporary computing hardware. Furthermore, due to its event-based characteristic, SNN inherently fits to process input from AER-based (address-event-representation) sensors that have low redundancy, low latency and high dynamic range, such as dynamic vision sensor (DVS) [19] and auditory sensor (silicon cochlea) [20]. A recent work [28] reported that spiking stereo neural network implementation consumes roughly one order of magnitude less energy than a micro-controller implementation based on classic sum-of-absolute-differences (SAD) algorithm.

Currently, one main challenge of SNN is to find an efficient training algorithm that can overcome the discontinuity of spiking and achieve comparable performance to ANNs. Conversion method, i.e., training a conventional ANN and building a conversion algorithm to map the weights to an equivalent SNN achieves the best performance by far. However, the conversion of a very deep network has never been addressed before.

In this paper, we investigate the learning of deep SNN based on residual network [11], a cutting-edge CNN architecture that has achieved great performance across many datasets and allows network to go extreme deep. We convert a pre-trained residual network to its spiking version with the assumption that the converted ResNet still has its original advantages. In order to scale continuous-valued

activations to fit SNN, we develop the shortcut normalisation to scale shortcut connection and maintain unit max firing rate across the SNN, i.e., neurons at each layer can reach the theoretically max firing rate (a spike is fired at each time step). We also propose a layer-wise compensation approach to improve the approximation by reducing sampling error at each layer.

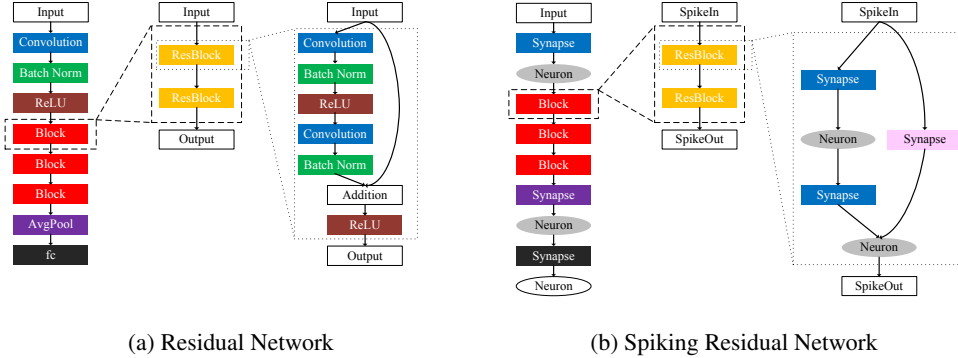


Figure 1: Illustration of spiking residual network architecture

## 2 Related Work

Due to the indifferentiability in the spiking mechanism of SNN, it is hard to directly apply classic learning methods of ANNs, such as backpropagation, to SNNs. In order to address this problem, researchers have devised a wide variety of learning algorithms to build SNNs. One approach is to directly learn from spikes with backpropagation-like algorithm by approximating the threshold function with linearity. For example, early work such as the *Spikeprop* [2] assumes the potential function to be differentiable for a small region around firing time. More recently, Lee et al. [17] demonstrated learning SNN with stochastic gradient descent (SGD) by regarding membrane potentials of spiking neurons as differentiable signals and discontinuities at spike times as noise.

Another approach is to learn with spike-timing-dependent plasticity (STDP) [1], a biologically plausible approach. In [22, 23], STDP has been proven able to select features in an unsupervised manner. Improved STDP algorithms such as rectangular STDP [30] and exponential STDP [4] can achieve competitive performance on MNIST dataset with a simple two-layer network.

The study of converting a pre-trained CNN to its equivalent SNN began as Perez-Carrasco et al. [29] introduced an approach to obtain the weights of SNN by scaling the weights of its CNN counterpart in accordance with the parameters of Leaky Integrate-and-Fire (LIF) [10] spiking neuron. O’Connor et al. [27] proposed a method to train deep brief network (DBF) with Siebert neuron which can approximate the firing rate of LIF spiking neuron. Consequently, the DBF trained with classic contrastive divergence algorithm can be better mapped to a spiking DBF. Esser et al. [7] considered the continuous value in ANNs as the probability of spikes and discrete synapses. They trained an ANN with backpropagation and mapped it to spiking network on TrueNorth by approximating the possibility of firing (activation) with complementary cumulative distribution function of a Gaussian distribution. Afterwards, Hunsberger et al. [13] demonstrated another way to approximate LIF neuron with SoftLIF activation function and that adding noise during training can improve the tolerance of errors caused by approximation. In [3], Cao et al. made use of the tight relation between commonly used ReLU activation function and the threshold function in spiking neuron, since ReLU eliminates all negative activations and continuous value in ANNs equals the firing rate of neurons in SNN. Further improvement was done by Diehl et al. [5]. They presented a weight normalisation method to adjust firing rates so as to avoid under firing or over firing. Then, Neil et al. [25] converted several successful techniques in ANNs, such as sparse coding, dropout, stacked auto-encoder (SAE) to SNN version. Diehl et al. [6] extended previous work to RNNs by utilising synaptic delay. Esser et al. [8] showed us that proper choices of network structure, neurons, network input and weights can optimise CNNs to meet the restrictions on TrueNorth. Lately, Rueckauer et al. [31] demonstrated methods to convert common operations in ANNs such as max-pooling, softmax, batch-normalization and Inception-modules to their spiking equivalents. We note that previous research primarily focus on

relatively shallow network which usually has less than 20 convolutional layers while contemporary ANNs can reach hundreds of layers or even a thousand layers.

### 3 Building Spiking ResNet

Originally, residual network was proposed to address the degradation problem of deep network. Stating from the insight that a deep network constructed by adding identity mapping layers will not perform worse than original shallow network, He et al. [11] let the stacked nonlinear layers approximate the mapping of  $\mathcal{F}(x) := \mathcal{H}(x) - x$ , where  $\mathcal{H}(x)$  is the desired underlying mapping. Then the original mapping becomes a residual mapping:  $\mathcal{H}(x) = \mathcal{F}(x) + x$ . They hypothesised that residual mapping is easier to be optimised with current solvers and verified their hypothesis with empirical evidence. Their experiments showed that residual network can obtain outstanding performance with exceptional depth. Inspired by their success, we assume that the spiking version of residual network inherits the advantages of ResNet and explore the uncharted area of learning very deep SNN with spiking residual network.

#### 3.1 Overview of Conversion

In Figure 1, we present the scheme for converting residual network to spiking residual network. By assuming that ReLU unit can approximate the firing rate of spiking IF neuron, we replace ReLU neuron in residual network (Figure 1(a)) with IF neuron and directly map the weights to spiking residual network (Figure 1(b)). Biases are also directly mapped to spiking residual network and analogue input are encoded into spike train at first hidden layer, by viewing these two as constant input current injected to spiking neuron [31]. As for batch normalisation layer [14], it regulates input to zero mean and unit variance, i.e.,

$$y = \frac{\gamma(x - \mu)}{\sigma} + \beta \quad (1)$$

where  $\mu$  is the mean,  $\sigma$  is the variance,  $\beta$  and  $\gamma$  are two learnable parameters. If we replace  $x$  with  $Wx + b$ , output from previous convolutional layer (Eq.(2)),

$$y = \left(\frac{\gamma W}{\sigma}\right)x + \left(\frac{\gamma(b - \mu)}{\sigma} + \beta\right) \quad (2)$$

we convert batch normalisation layer by directly regulating the weight and bias of previous convolutional layer to  $\widetilde{W} = \frac{\gamma W}{\sigma}$  and  $\widetilde{b} = \frac{\gamma(b - \mu)}{\sigma} + \beta$ . After the weights are mapped to spiking network, weight normalisation is applied to scale the continuous-valued activations to a region of  $[0, r_{max}]$ , where  $r_{max}$  is the unit max firing rate as spiking neuron can fire no more than one spike at each time step. Weights are jointly normalised by  $\overline{W} = \frac{\lambda^{l-1}}{\lambda^l} W$  and biases are normalised by  $\overline{b} = \frac{1}{\lambda^l} b$ . Here,  $\lambda^l$  is the max 99.9% activation at layer  $l$  instead of the actual max activation as using the actual max activation is more prone to be susceptible to outliers [31].

Two problems arose during the conversion process. First, different from traditional linear structure, the structure of spiking residual network is a directed acyclic graph. In order to scale the activations appropriately, we must also take its input from the shortcut connection into consideration as the conversion introduces new synaptic weights in shortcuts (Figure 1(b)). Second, we found that the sampling error caused by discretisation can no longer be ignored as it has become a major factor responsible for the degradation of performance in very deep SNN. The two issues will be solved in Section 3.2 and 3.3 respectively.

#### 3.2 Shortcut normalisation

Here, we consider the case of a basic residual block in Figure 2. We let  $max_1, max_2, max_3$  denote max activations in ReLU1, ReLU2 and ReLU3, respectively.  $W_1, b_1, W_2, b_2$  are weights and biases in Conv1 and Conv2. For this block, its input is  $x$  from ReLU1 and its output is

$$y = W_2(W_1x + b_1) + b_2 + x \quad (3)$$

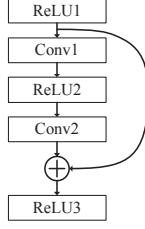


Figure 2: Basic Residual Block

In order to maintain unit max firing rate, we normalise output of block by its max activation, i.e.,

$$y_{norm} = \frac{y}{max_3} = \frac{W_2(W_1x + b_1) + b_2 + x}{max_3} \quad (4)$$

According to weight normalisation, input, weights, biases are all rescaled as  $\bar{x} = \frac{1}{max_1}x$ ,  $\bar{W}_1 = \frac{max_1}{max_2}W_1$ ,  $\bar{b}_1 = \frac{1}{max_2}b_1$ ,  $\bar{W}_2 = \frac{max_2}{max_3}W_2$ ,  $\bar{x} = \frac{1}{max_1}x$ . We suppose shortcut also have to be scaled with a parameter  $\lambda$  in accordance to normalisation in stacked layers. Output of residual block then becomes

$$\begin{aligned} y_{norm} &= \bar{W}_2(\bar{W}_1\bar{x} + \bar{b}_1) + \bar{b}_2 + \lambda\bar{x} \\ &= \frac{W_2(W_1x + b_1) + b_2}{max_3} + \frac{\lambda}{max_1}x \end{aligned} \quad (5)$$

By comparing Eq.(5) with Eq.(4),  $\lambda = \frac{max_1}{max_3}$  is derived. Therefore, in spiking residual network, shortcut in residual block should be normalised with  $\frac{input\_max\_activation}{output\_max\_activation}$ .

### 3.3 Compensation of Sampling Error

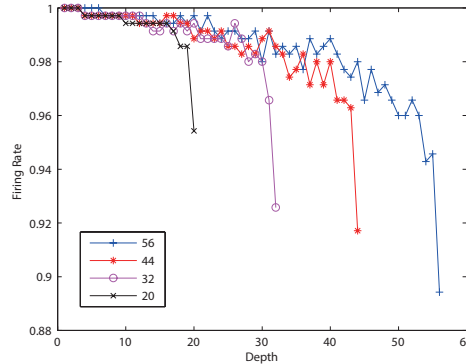


Figure 3: Change of max firing rate at each layer as network goes deep (4 networks with 20, 32, 44, 56 layers in total, respectively)

In an SNN converted from ANN, each layer receives a weighted sum of sampling error from previous layers and contributes its sampling error to the accumulated errors [31]. This situation is ascribable to discretisation and propagation of sampling errors. When the network is shallow, sampling errors do not have a significant impact on the performance of SNN. However, as network goes deep, the accumulating sampling errors reduce firing rate and degrade the performance of SNN notably. In Figure 3, we demonstrate the change of max firing rate at each layer in spiking residual network of depth 20, 32, 44 and 56, across 10000 training samples randomly selected from the training set of CIFAR-10 dataset. Though the max firing rate at each layer is supposed to have unified value after

joint normalisation is applied, the actual max firing rate declines as network goes deep. The deeper the network is, the lower the max firing rate at the final layer will be. To address this problem, we assume that sampling error can be reduced by slightly enlarge the weights at each layer. Then we apply a compensation factor  $\lambda$  to each layer of the network to reduce sampling errors by slightly enlarge the weights. Compensation factor  $\lambda$  is searched in a region of  $(1, \tau_{max})$ , where  $\tau_{max}$  is the reciprocal of max firing rate at the last layer.

## 4 Experimental Results

To validate our conversion methods, we evaluate the performance of spiking residual network on MNIST [16], CIFAR-10 and CIFAR-100 [15]. Here, input data is first preprocessed by feature standardisation. In our experiments, we employ the basic residual block: a stack of two  $3 \times 3$  convolutional layers and a shortcut connection. We also use a simple dataset augmentation [11] on CIFAR-10 and CIFAR-100, by padding 4 pixels on each side of the image and randomly crop from the padded image with a window of  $32 \times 32$ . In addition, we also horizontally flip the image at a chance of 50%. Residual networks are trained with standard stochastic gradient descent (SGD) with a momentum of 0.9. We first warm up the network with the initial learning rate 0.01 for 3 epochs. Then we set the learning rate back to 0.1 and divide the learning rate by 10 after 83th, 93th epoch. Training is finished at 113th epoch. All experiments are conducted with deep learning library MatConvNet [33].

### 4.1 Comparison with Other Deep SNNs

In Table 1, we present a summary of our results achieved on MNIST, CIFAR-10, CIFAR-100, along with comparison with the performance of other deep SNNs. The depth here is defined by considering all layers with learnable weight in neural network, i.e., convolutional and fully connected layers. On all three datasets, our spiking ResNet achieved better performance than other deep SNNs. On MNIST dataset, we achieved loss-less conversion of ResNet-8 and obtained an accuracy of 99.59%. We did not conduct experiment with deeper network on MNIST as we believe that a shallow work is adequate to learn the hidden mapping behind these handwritten digits. On CIFAR-10 dataset, highest performance, 92.37%, was achieved by spiking ResNet-44, which is the deepest feedforward SNN by far. The accuracy of original ResNet-44 is 92.85% and the accuracy loss caused by conversion is 0.48%, which is very low in comparison with other deep SNNs. On CIFAR-100 dataset, spiking ResNet-44 also achieved good performance, with an accuracy of 68.56%. The conversion process induced a decrease in accuracy by 1.62%.

Table 1: Comparison with other conversion methods on MINIST, CIFAR-10, and CIFAR100.

Dataset	Depth	ANN	SNN	Accuracy Loss
MNIST[5]	3	99.14%	99.12%	0.02%
MNIST[31]	4	99.44%	99.44%	0%
<b>MNIST(ours)</b>	8	<b>99.59%</b>	<b>99.59%</b>	<b>0%</b>
CIFAR-10[3]	5	79.12%	77.43%	1.69%
CIFAR-10[13]	5	85.97%	83.54%	2.43%
CIFAR-10[8]	16	N/A	89.32%	N/A
CIFAR-10[31]	9	91.91%	90.85%	1.06%
<b>CIFAR-10(ours)</b>	44	<b>92.85%</b>	<b>92.37%</b>	<b>0.48%</b>
CIFAR-100[8]	16	N/A	65.48%	N/A
<b>CIFAR-100(ours)</b>	44	<b>70.18%</b>	<b>68.56%</b>	<b>1.62%</b>

### 4.2 Experiment on Shortcut Normalisation

To evaluate the effectiveness of shortcut normalisation, we train residual networks of depth 20, 32, 44, 56, 110 on CIFAR-10 and convert them to spiking residual network with or without shortcut normalisation. Table 2 presents the recognition accuracy of original residual network and corresponding spiking residual network with or without shortcut normalisation. Across all depths, SNN with

shortcut normalisation performs better than SNN without shortcut normalisation. The difference between their performance goes from 2.34% to 6.32%, 7.42%, 8.31%, 8.59% as depth increases from 20 to 32, 44, 56, 110. As network goes deeper, SNN without shortcut normalisation suffers more performance loss than SNN with shortcut normalisation. Besides, the performance of SNN with shortcut normalisation is quite stable with depth of 20, 32, 44, 56. At depth 20, the performance drops by only 0.20% after conversion.

Table 2: Classification accuracy of residual network and spiking residual network with or without shortcut normalisation on CIFAR-10

Depth	ANN	SNN- $\alpha^1$	ANN-to-SNN- $\alpha$ loss	SNN- $\beta^2$	ANN-to-SNN- $\beta$ loss
20	91.99%	89.45%	2.54%	91.79%	0.20%
32	92.66%	85.38%	7.28%	91.70%	0.96%
44	92.85%	84.56%	8.29%	91.98%	0.87%
56	92.99%	83.33%	9.66%	91.64%	1.35%
110	93.47%	79.23%	14.24%	87.82%	5.65%

<sup>1</sup> without shortcut normalisation

<sup>2</sup> with shortcut normalisation

### 4.3 Spiking ResNet vs Conventional Spiking CNN

To verify the advantages of residual mapping in conversion from ANNs to SNNs, we here assess the performance of spiking ResNet and conventional spiking CNNs. Comparison between Spiking ResNet and conventional spiking CNN on CIFAR-10 is shown in Figure 4. The plain network, i.e., network without shortcut connection, is converted with the established conversion techniques from a VGG-like [32] network (Figure 5). At depth 20, the performance of plain network drops by 1.97% after conversion. However, as the depth increases, performance loss goes up to 6.11%, 28.60%, 41.75% at depth 32, 44, 56. The drastic drop of performance at depth implies that conversion results in a huge amount of errors in deep plain network. Meanwhile, performance loss in residual network stays below 2% across four different depths. We believe this phenomena is attributed to the difference in their architectures.

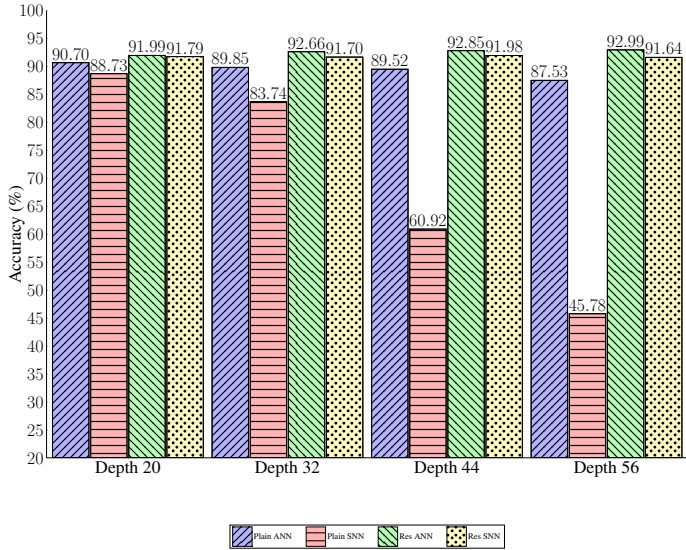


Figure 4: Comparison of conversion efficiency between plain networks and residual networks on CIFAR-10

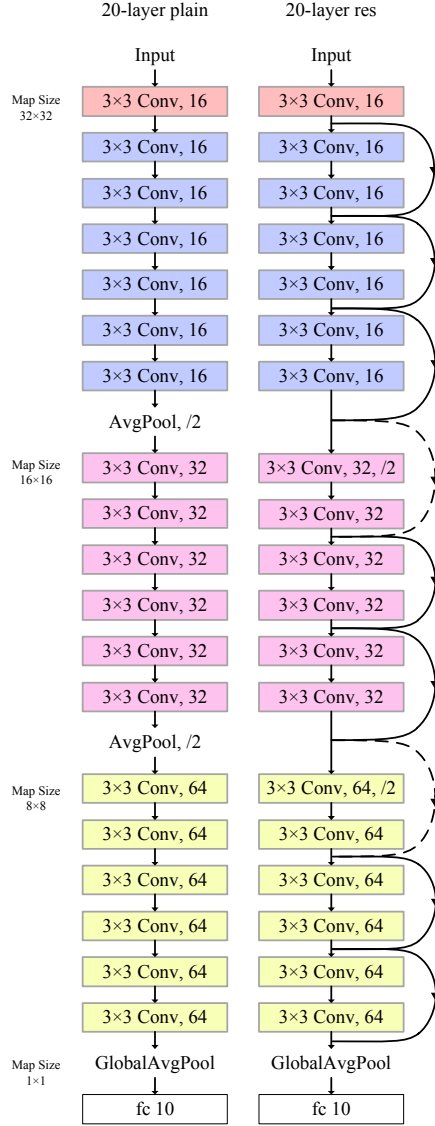


Figure 5: Architectural comparison of plain ANN and residual ANN

Table 3: Experimental results of error compensation approach on CIFAR-10

Depth	plain network		residual network	
	SNN	SNN with comp.	SNN	SNN with comp.
20	88.73%	89.40%	91.79%	91.82%
32	83.74%	86.12%	91.70%	92.04%
44	60.92%	69.12%	91.98%	92.37%
56	45.78%	58.51%	91.64%	92.33%

#### 4.4 Experiment on Error Compensation

In Table 3, we applied our compensation approach to both spiking residual network and spiking network converted from conventional CNN (plain network). For plain network, the performance of SNN improved by 0.67%, 2.38%, 8.20%, 12.73% at depth 20, 32, 44, 56, respectively. For residual network, the performance of SNN improved by 0.03%, 0.34%, 0.39%, 0.69% at depth 20, 32, 44, 56.

The variation of the improvement by compensation at different depths also implies that more errors are accumulated in a deeper network. We also note that improvements on plain network are much higher than those on residual network, which indicates that conversion process induces more errors in plain network than in residual network. This result further suggests that plain architecture is more prone to be affected by sampling errors.

## 5 Conclusion and Discussion

For the first time, we explored building a very deep SNN – Spiking ResNet. We proposed an efficient framework to convert a trained deep residual network to its equivalent spiking deep residual network. Meanwhile, we introduced shortcut normalisation to adapt the shortcut connection for maintaining unit max firing rate across the network, and presented an approach to decrease sampling error by apply a compensation factor to weights at each layer. Experiments were conducted on MNIST, CIFAR-10, and CIFAR-100, and the results demonstrated that our method achieved the state of the art.

Furthermore, we found that the accumulating sampling error caused by discretisation remains a crucial problem for deep SNNs converted from ANNs. Though deep ANNs often give better performance before conversion, this benefit of deeper network can be totally compromised due to the increasing sampling error as network goes deeper. This problem calls for a better approximation method.

In our experiments, we also found that residual mapping can stabilise the performance of Spiking ResNet. Some underlying connections may exist between residual network and biological neural network. In [18], Liao et al. suggest that residual networks are equivalent to RNNs and RNNs are biologically plausible models of vision cortex. As we know, the biological network is highly fault-tolerant and is able to shape its weights and complex structure during learning. Biological findings indicate that it takes much less time to alter the weights of synapse than creating a new synaptic connection. With residual mapping, we can re-train falsely learned knowledge by simply suppressing synaptic weights in stacked layers, without introducing new synaptic connection. Moreover, the shortcut connection also enables network to do inference with reference to output from much lower layer. In [12], pre-activation structure achieved better performance than original residual block. It is worthy to note that if we interpret the addition as integration of incoming information, then each residual block in pre-activation structure is actually integrating the output information from every residual block that is lower than itself, which is similar to the integration of high level knowledge and low level knowledge in biological system. Therefore, we believe there is some intrinsic biological plausibility in residual mapping.

In our future work, we will try to improve the approximation and explore the conversion of versatile ANN architectures, as well as understanding their hidden biological plausibility.

## References

- [1] BI, G.-Q., AND POO, M.-M. Synaptic modifications in cultured hippocampal neurons: dependence on spike timing, synaptic strength, and postsynaptic cell type. *Journal of neuroscience* 18, 24 (1998), 10464–10472.
- [2] BOHTE, S. M., KOK, J. N., AND LA POUTRE, H. Error-backpropagation in temporally encoded networks of spiking neurons. *Neurocomputing* 48, 1 (2002), 17–37.
- [3] CAO, Y., CHEN, Y., AND KHOSLA, D. Spiking deep convolutional neural networks for energy-efficient object recognition. *International Journal of Computer Vision* 113, 1 (2015), 54–66.
- [4] DIEHL, P. U., AND COOK, M. Unsupervised learning of digit recognition using spike-timing-dependent plasticity. *Frontiers in computational neuroscience* 9 (2015).
- [5] DIEHL, P. U., NEIL, D., BINAS, J., COOK, M., LIU, S.-C., AND PFEIFFER, M. Fast-classifying, high-accuracy spiking deep networks through weight and threshold balancing. In *2015 International Joint Conference on Neural Networks (IJCNN)* (2015), IEEE, pp. 1–8.
- [6] DIEHL, P. U., ZARRELLA, G., CASSIDY, A., PEDRONI, B. U., AND NEFTCI, E. Conversion of artificial recurrent neural networks to spiking neural networks for low-power neuromorphic



- hardware. In *Rebooting Computing (ICRC), IEEE International Conference on* (2016), IEEE, pp. 1–8.
- [7] ESSER, S. K., APPUSWAMY, R., MEROLLA, P., ARTHUR, J. V., AND MODHA, D. S. Back-propagation for energy-efficient neuromorphic computing. In *Advances in Neural Information Processing Systems* (2015), pp. 1117–1125.
- [8] ESSER, S. K., MEROLLA, P. A., ARTHUR, J. V., CASSIDY, A. S., APPUSWAMY, R., ANDREOPOULOS, A., BERG, D. J., MCKINSTRY, J. L., MELANO, T., BARCH, D. R., ET AL. Convolutional networks for fast, energy-efficient neuromorphic computing. *PNAS* (2016), 201604850.
- [9] FURBER, S. B., GALLUPPI, F., TEMPLE, S., AND PLANA, L. A. The spinnaker project. *Proceedings of the IEEE* 102, 5 (2014), 652–665.
- [10] GERSTNER, W., AND KISTLER, W. M. *Spiking neuron models: Single neurons, populations, plasticity*. Cambridge University Press, 2002.
- [11] HE, K., ZHANG, X., REN, S., AND SUN, J. Deep residual learning for image recognition. In *CVPR* (2016), pp. 770–778.
- [12] HE, K., ZHANG, X., REN, S., AND SUN, J. Identity mappings in deep residual networks. In *European Conference on Computer Vision* (2016), Springer, pp. 630–645.
- [13] HUNSBERGER, E., AND ELIASMITH, C. Spiking deep networks with lif neurons. *arXiv preprint arXiv:1510.08829* (2015).
- [14] IOFFE, S., AND SZEGEDY, C. Batch normalization: Accelerating deep network training by reducing internal covariate shift. In *International conference on machine learning* (2015), pp. 448–456.
- [15] KRIZHEVSKY, A., AND HINTON, G. Learning multiple layers of features from tiny images.
- [16] LECUN, Y., BOTTOU, L., BENGIO, Y., AND HAFFNER, P. Gradient-based learning applied to document recognition. *Proceedings of the IEEE* 86, 11 (1998), 2278–2324.
- [17] LEE, J. H., DELBRUCK, T., AND PFEIFFER, M. Training deep spiking neural networks using backpropagation. *Frontiers in Neuroscience* 10 (2016).
- [18] LIAO, Q., AND POGGIO, T. Bridging the gaps between residual learning, recurrent neural networks and visual cortex. *arXiv preprint arXiv:1604.03640* (2016).
- [19] LICHTSTEINER, P., POSCH, C., AND DELBRUCK, T. A 128 x 128 120db 30mw asynchronous vision sensor that responds to relative intensity change. In *Solid-State Circuits Conference, 2006. ISSCC 2006. Digest of Technical Papers. IEEE International* (2006), IEEE, pp. 2060–2069.
- [20] LIU, S.-C., VAN SCHAIK, A., MINCTI, B. A., AND DELBRUCK, T. Event-based 64-channel binaural silicon cochlea with q enhancement mechanisms. In *2010 IEEE International Symposium on Circuits and Systems* (2010), IEEE, pp. 2027–2030.
- [21] MAASS, W. Networks of spiking neurons: the third generation of neural network models. *Neural networks* 10, 9 (1997), 1659–1671.
- [22] MASQUELIER, T., AND THORPE, S. J. Unsupervised learning of visual features through spike timing dependent plasticity. *PLoS Comput Biol* 3, 2 (2007), e31.
- [23] MASQUELIER, T., AND THORPE, S. J. Learning to recognize objects using waves of spikes and spike timing-dependent plasticity. In *The 2010 International Joint Conference on Neural Networks (IJCNN)* (2010), IEEE, pp. 1–8.
- [24] MEROLLA, P. A., ARTHUR, J. V., ALVAREZ-ICAZA, R., CASSIDY, A. S., SAWADA, J., AKOPYAN, F., JACKSON, B. L., IMAM, N., GUO, C., NAKAMURA, Y., ET AL. A million spiking-neuron integrated circuit with a scalable communication network and interface. *Science* 345, 6197 (2014), 668–673.
- [25] NEIL, D., PFEIFFER, M., AND LIU, S.-C. Learning to be efficient: algorithms for training low-latency, low-compute deep spiking neural networks. In *the 31st Annual ACM Symposium on Applied Computing* (2016), ACM, pp. 293–298.
- [26] NING, Q., HESHAM, M., FABIO, S., AND DORA, S. A reconfigurable on-line learning spiking neuromorphic processor comprising 256 neurons and 128k synapses. *Frontiers in Neuroscience* 9 (2015), 141.

- [27] O’CONNOR, P., NEIL, D., LIU, S., DELBRUCK, T., AND PFEIFFER, M. Real-time classification and sensor fusion with a spiking deep belief network. *Frontiers in Neuroscience* 7 (2013), 178–178.
- [28] OSSWALD, M., IENG, S.-H., BENOSMAN, R., AND INDIVERI, G. A spiking neural network model of 3d perception for event-based neuromorphic stereo vision systems. *Scientific Reports* 7, 40703 (2017).
- [29] PÉREZ-CARRASCO, J. A., ZHAO, B., SERRANO, C., ACHA, B., SERRANO-GOTARREDONA, T., CHEN, S., AND LINARES-BARRANCO, B. Mapping from frame-driven to frame-free event-driven vision systems by low-rate rate coding and coincidence processing—application to feedforward convnets. *IEEE transactions on pattern analysis and machine intelligence* 35, 11 (2013), 2706–2719.
- [30] QUERLIOZ, D., BICHLER, O., DOLLFUS, P., AND GAMRAT, C. Immunity to device variations in a spiking neural network with memristive nanodevices. *IEEE Transactions on Nanotechnology* 12, 3 (2013), 288–295.
- [31] RUECKAUER, B., LUNGU, I.-A., HU, Y., PFEIFFER, M., AND LIU, S.-C. Conversion of continuous-valued deep networks to efficient event-driven networks for image classification. *Front. Neurosci.* 11: 682. doi: 10.3389/fnins (2017).
- [32] SIMONYAN, K., AND ZISSERMAN, A. Very deep convolutional networks for large-scale image recognition. *In ICLR* (2015).
- [33] VEDALDI, A., AND LENC, K. Matconvnet: Convolutional neural networks for matlab. *In Proceedings of the 23rd ACM international conference on Multimedia* (2015), ACM, pp. 689–692.